Egypt. J. Chem. **Vol. 65,** No. SI:13B pp. 745-757 (2022)

Egyptian Journal of Chemistry

http://ejchem.journals.ekb.eg/

Preparation, Characterization and Water Treatment Application of Electro-spun Polyamide 6 Nanocomposite

Ahmed R Abdelhafiz [1], Wael S Mohamed [2], Sabrnal H El Hamouly [3], Nabila A Maziad [4], Mahmmoud S Abd Elmonem [5]

[1] *Public Treasury and Mint Authority, Ministry of finance, Cairo,Egypt.*
[2] *Department of Polymers and Pigments, National Research Centre, Giza, Egypt.*
[3] *Polymer Laboratory, Department of Chemistry, Faculty of Science, Menoufia University, Shibin el Kom, Egypt.*
[4] *Department of Polymer Chemistry, National Center for Radiation Research and Technology (NCRRT),Egyptian Atomic Energy Authority ,Cairo, Egypt.*
[5] *Egyptian Drug Authority (EDA), Giza, Egypt.*

Abstract

This study aims to synthesize Polyamide 6 nanofibrous membrane of low molecular weight (PA6) using an electrospinning technique with a concentration of 30% (wt/v) and Polyamide 6 nanofibers containing calcium oxide nanoparticles (PA6/CaO), which were obtained with a CaO concentration of 1% (wt/wt). Scanning electron microscopy (SEM) was used to examine the structure of the electrospun nanofibers, which showed smooth and continuous electrospun nanofibers with a nanofibrous diameter of around 53 nm, and CaO nanoparticles were distributed through the nanofibers with a slight increase in the nanofibrous diameter.The surfaces of the obtained PA6 and PA6/CaO nanofibers were modified by grafting polymerization with acrylic acid AA, with various synthetic parameters such as reaction temperature, monomer concentration, initiator concentration, and emulsifier concentration. The obtained results show that as the concentrations of monomer, initiator, and temperature increased, the grafting yield increased at first, then decreased, but it kept increasing as the emulsifier concentration was increased. The characterization of the obtained graft nanofibers was carried out using Fourier Transform Infrared Spectroscopy (FT-IR), Thermo Gravimetric Analysis (TGA), and Differential Scanning Calorimetry (DSC). The effects of pH, initial concentration, temperature, and contact time on the removal of heavy metals (Co^{2+}, Cr^{6+}) from water solution were investigated, and it was observed that a polyamide6/CaO nanofibrous membrane grafted with AA could adsorb Co^{2+} more than Cr^{6+}. While the optimum conditions for the removal were observed at an initial concentration of 10 ppm, pH 5 at 150 min under 30 °C.

Keywords: *Electro-spinning, Water Treatment, Nanocomposite, Nanoparticles, Nylon 6, Heavy metal Removal*

Introduction

Electrospinning has attracted a lot of attention because it is a simple and effective way to produce nanofibers out of a variety of polymers or polymers with non-spinnable materials, resulting in a wide range of functional membranes which can be applied in the field of biomedical and environmental applications [1-4]. Electro spinning is a technique for preparing nanofibers from polymeric liquids using a high electric field [5]. Electrospun non-woven webs of ultrafine fibers can be made from both polymer solutions and melts. Between a nozzle and a collector, an electrostatic field is created, with electric force being employed to eject the polymer solution from the nozzle towards the collector. The solvent evaporates from the polymer jet, however instabilities in the jet occur, resulting in nano-sized fiber widths and affecting the shape of the producing fibers [6].

A number of parameters can influence the morphology of fibres during the electrospinning of a polymer solution. These variables can be classified into three categories: 1) the polymer solution (viscosity, concentration, conductivity, and surface tension), 2) the process (collection distance, applied electrostatic potential, and feed rate), and 3) ambient parameters (relative humidity, temperature, and velocity of the surrounding air in the spinning chamber) [7, 8]. The nanofibers have a larger surface area, porosity, penetrability, and interaction with other chemicals, making the sorption process more acceptable and effective for the removal of metals and dyes in water treatment [9, 10].

Polyamide 6 is an engineering resin composed of amide groups connected by methylene sequences that can be electrospun into extremely good fibers with excellent mechanical, thermal, and chemical properties [11].

*Corresponding author e-mail: ahmed_rabdelhafiz@yahoo.com.; (Ahmed R. Abdel Hafiz).
Receive Date: 27 June 2022, Revise Date: 06 November 2022, Accept Date: 01 September 2022
DOI: 10.21608/EJCHEM.2022.146953.6395

Grafting various vinyl monomers, such as acrylate, acrylic, and methacrylic acid (MAA), onto the surface of polyamide 6 can impart a variety of functional groups onto a hydrophobic polymer backbone and modify the physical and chemical properties of the polymer surface to have a better affinity with water [12-14].

Heavy metal toxicity is a major threat to public health and human-altered environments all over the world. They primarily act as environmental contaminants, and their long-term retention in the environment presents a major hazard to animal and human health. The majority of heavy metal pollutants are usually focused on cobalt and chromium, which are poisonous and carcinogenic and may cause health problems in humans [15, 16]. Adsorption has recently received much attention as a method for removing heavy metal ions from water and waste water. Chemisorptions are a new type of adsorption that has a high adsorption capacity (over 90% removal), a quick adsorption equilibrium, and is easy to regenerate [17].

The present work aims to produce nanofibrous membranes of PA6 and PA6/CaO nanocomposite and modify the surface of the obtained nanofibrous membranes by grafting polymerization with acrylic acid AA as a monomer and using potassium persulfate as an initiator with a variation of synthetic parameters. The Optimal grafting nanofibrous is utilized to remove heavy metals (Co^{2+}, Cr^{6+}) from simulated water solutions. And evaluated through the influence of initial metal concentration, pH value, contact time, and temperature.

Experimental

Materials

Polyamide 6 with low molecular weight was obtained from Sigma-Aldrich, Germany. Formic acid (85%) was purchased from ADWIC, El Nasr pharmaceutical chemicals co., Egypt. Calcium oxide CaO nanoparticle was from SD Fine chem limited co., Acrylic acid was obtained from Merck Schuchardt, Germany. Potassium persulfate (PPS) was from Modern Lab of purity > 98% and Texapon N70 (sodium lauryl ether sulfate (SLES)) was provided from BASF chemicals company,Cobalt (II) Nitrate hexahydrate 97% was obtained from Loba Chemie ,Potassium dichromate was Obtained from QualiKems.

Methods

Preparation of polymer PA6 and pa6/CaO nanocomposite solutions

Polyamide 6 was dissolved in formic acid (85%) at a concentration of 30% (w/v) under magnetic stirring at room temperature to obtain a clear and homogeneous solution for production of neat PA6 fibers. In order to prepare PA6/CaO nanocomposite nanofibers, first, PA6 was dissolved in formic acid at 30 % (w/v) at room temperature for 1h to obtain a clear solution, then CaO nanoparticle was added with 1% to PA6 (w/w) ratio and finely dispersed by a magnetic stirrer at room temperature for 12 hours, then bath sonicated for 1h (Ultrasonic bath MTI, model UD50SH-2LQ, 50W) to assure homogenous dispersion.

Electrospinning Process

The electrospinning experiments were conducted at room temperature. The polymer solution was injected into a 1-mL syringe fitted with a metallic needle (20 G). A piece of aluminum foil operated as a collector at a distance of 10 cm from the needle tip. A high voltage power supply was adjusted using a Glassman High Voltage Series (voltage range 0-20 kV) to charge the spinning PA6 solutions by connecting the emitting electrode of positive polarity to the nozzle (the needle) and the grounding electrode to the collective screen. The polymer jets generated from the needle by high voltage flew to the collector and formed the nanofiber mesh. Finally, the electrospun samples were dried overnight at 40°C. The voltage Syringe Pump Series 100 regulated the flow rate of the solution at 0.2 ml/h. Electrospinning was done at ambient temperature and at a relative humidity (RH) of 40 ± 2% [18].Using a scanning electronic microscope (SEM), the morphologies of the dried nanofibrous membrane were examined.

Grafting polymerization procedure

1g in weight of PA6 and PA6/CaO electrospun nanofibrous were placed separately in a stoppered glass vessel containing 20 mL distilled water, Potassium persulfate (PPS) as an initiator ($1x10^{-3}$ mol/l), and 1% sodium lauryl ether sulfate (SLES) as a emulsifier, then the vessel was gently shaken for 10 minutes with a thermostatic shaker water bath (HWT-10C with temperature range up to 100ºC and speed up 200 rpm, China). 5% Acrylic Acid (AA) monomer was added to the mixture. Then the temperature was adjusted to 60ºC and the graft polymerization was allowed to continue under shaking for the period specified (4 hr). After that, the homopolymer and unreacted components were removed from the modified electrospun fiber by washing it with distilled water. The obtained grafted copolymer PA6-g-AA and PA6/ CaO-g-AA nanofibrous membranes were then dried at 40ºC for 12h and under several grafting variable conditions the grafting yield percentage has been calculated for all factors which affecting the grafting process to determine the optimum yield using the below Equation:

$$\textbf{Grafting yield (\%)} = [(W_g - W_o)/ Wo] \times 100$$

Where w_g and w_o are the weights of the electrospun nanofibrous membrane after and before grafting, respectively [19]. Scanning Electronic Microscope (SEM) and Transmittance Reflectance-FTIR were used to investigate the dried grafted electrospun fiber.

Swelling behaviour

Swelling of The obtained grafted copolymer PA6-g-AA and PA6/CaO-g-AA nanofibrous membranes were carried out in 25 ml distilled water at room temperature. The weight of dry grafted sample was estimated then placed in the swelling medium [20]. At specific time intervals, the membranes taken out from the swelling medium, drained, and wiped with tissue paper to remove excess water. The weight of swollen sample was estimated and the swelling ratio was calculated from using the below Equation: [21].

$$\textbf{Degree of Swelling \%} = [(W_t - W_0) / W_0] \times 100$$

Where W_0 and W_t are the initial weight of the dry sample and swollen sample, respectively at estimated time points.

Adsorption procedure for heavy metals

During the study, two stocks of heavy metal solutions for simulated wastewater were prepared, with different concentrations of cobalt nitrate and potassium dichromate from 10 to 200 ppm for both heavy metals. The adsorption capacity of grafted fibers for Co^{2+} and Cr^{6+} ions was investigated using a batch procedure and a single element method.

In a 100 mL Erlenmeyer flask, add 20 mL metal ion solution. Chemically modified PA6/CaO-gAA nanofibrous samples (30 mg) were soaked in a pH-adjusted solution. At 30° C, the contents were shaken at 200 rpm for a predetermined amount of time. The effects of the pH, initial metal concentration, temperature, and contact time on the removal of heavy metals were investigated. The samples were filtered at the end of the experiment, and the ion concentration of the filtrates was evaluated with a UV spectrophotometer after the solution was filtered. The following formulae were used to compute the removal percentage (R %):

$$R\ \% = [(C_i - C_r) / C_i] \times 100$$

Where:

C_i and C_r are the initial and final concentrations of the investigated metal ion in the solution (ppm).

Characterizations

Scanning Electronic Microscope (SEM)

The morphologies of the dried electrospun PA6 and PA6/CaO nanofibers samples before and after grafting were investigated using a scanning electronic microscope SEM (a QUANTA FEG250 model-Japan). By fixing a small piece of fiber to a small cupper plate and applying a light gold layer to the fiber's surface for 1 minute. The photos were obtained with various magnifications at HV of 20.00KV and an appropriate one was chosen. The diameter of the nanofibers produced was measured.

Fourier Transform Infrared ATR-FTIR Spectroscopy

The graft copolymers PA6-g-AA and PA6/CaO-g-AA after washing and drying was further characterized by FTIR (Vertex 80V Bruker) in the range from 4000 to 400 cm^{-1}. Using the technique of Attenuated Total Reflectance ATR. Where an ATR is a sampling technique used in conjunction with infrared spectroscopy that allows samples to be examined directly in the solid or liquid state without further preparation and performs by measuring changes in an internally reflected IR beam when it comes into contact with the sample's surface [22].

Thermogravimetric analysis (TGA)

TGA was carried out to evaluate PA6 and PA6/CaO nanofibers before and after grafting samples using Themys One+ instrument. The thermal stabilities of the samples were heated under nitrogen at the rate of 10 ℃/min in the range from 50℃ to 600 ℃

Differential Scanning Calorimetry (DSC)

The DSC thermogram of PA6 and PA6/CaO nanofibers before and after grafting were measured using the DSC131 Evo Setaram instrument. The nanofibers were heated between 50 and 600 °C at 10 °C/min. [23].

UV spectrophotometer

The ion concentration was determined by measuring the absorbance at 415 nm and 540 nm for cobalt and chromium, respectively, using an ultraviolet visible recording spectrophotometer Shimadzu spectrophotometer with double beam. All measurements were performed in triplicate.

Results and Discussion

PA6 and PA6/CaO electrospun nanofibrous membranes were successfully prepared by electrospinning polymer solution with PA6 concentration of 30% (wt/v) and CaO concentration of 1% (wt/wt). Previously, it was revealed that at those concentrations, smooth and continuous nanofibers form, resulting in a slight increase in nanofiber diameters [24].

Grafting PA6 fibbers with AA

On a laboratory scale, graft copolymerization of AA onto PA-6 fibers was carried out using SLES as a emulsifier in the presence of PPS as an initiator. The effects of several parameters on the graft incorporate were examined. The best conditions for grafting PA-6 fibers have been reported. The main target of grafting the polyamide 6 with acrylic acid AA is to introduce carboxylic functional groups on the surface of the obtained electrospun fibers to o improve their affinity for metal removal.

Effect of monomer concentration

Figure 1 show that effect of monomer concentration on the grafting yield of PA6-gAA and PA6/CaO-gAA in the range of 5 to 25% at a constant initiator of $1x10^{-}$

^{3} (mol/l) and a constant emulsifier of 1% 60℃ for 4 hr grafting time.

As is evident, the grafting yield sharply increased with increasing monomer concentration till monomer concentration 15% achieves 25% and 41% grafting yield for PA6-gAA and PA6/CaO-gAA respectively, then the grafting yield starts to decrease. The initial rise in grafting yield was due to the fact that most of the monomer is utilized by the available free radical sites on the nanofibers backbone. Then, the decreasing of grafting yield after 15% monomer concentration could be caused by decreasing of the monomer penetration onto nanofibers due to the greater tendency for homopolymerization and increasing of the solution viscosity at high monomer concentrations which prevented the distribution of radicals and monomer to the active sites on the fibrous mat [25-27].

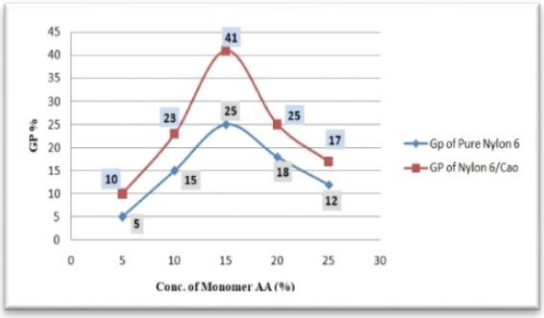

Fig 1. Effect of monomer concentration

Effect of emulsifier concentration

The relationship between the rates of grafting of AA onto PA6 and PA6/CaO with various concentrations of SLES as an emulsifier for was studied and illustrated in **figures 2** in the range of 0.5 to 2.5% at a constant monomer concentration of 15% and constant initiator of $1x10^{-3}$ (mol/l) at 60℃ for 4hr grafting time. The obtained data indicated that the rate of grafting of AA increased with an increasing the emulsifier concentration where the emulsifier powers were found to be highest at the concentration 2.5% , this can be attributed to the fact that an emulsifier plays an important role in increasing the swellability of nanofibers; consequently, increase the emulsification of the AA monomer led to form a homogeneous, miscible solution suitable for carrying out grafting polymerization more facilitation and penetration of free radicals inside the fiber backbone take place [28].

Effect of initiator Concentration

Figure 3 shows the effect of initiator concentration in the range of $0.5x10^{-3}$ to $2.5x10^{-3}$ (mol/l) at a constant monomer concentration 15% and emulsifier concentration 2.5% at 60℃ for 4hr grafting time.

From the figure, it is clear that, the grafting yield increased by increasing initiator concentration until it reached $1.5x10^{-3}$ (mol/l) achieves 43% and 67% grafting yield for PA6-gAA and PA6/CaO-gAA respectively and then the grafting yield starts to decrease. The increasing of grafting yield with increasing initiator concentration can be attributed to, the availability of a large number of active sites appropriate for forming polymer chains at high initiator concentrations.. The decreasing of grafting yield after $1.5x10^{-3}$ (mol/l) initiator is due to the free radicals reacted with the filament macro-radical and forming homopolymer chains at high initiator concentration, resulting in termination or combination reactions, decreasing the grafting yield. [29].

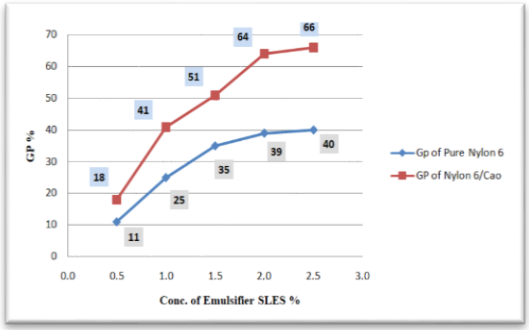

Fig 2. Effect of emulsifier concentration

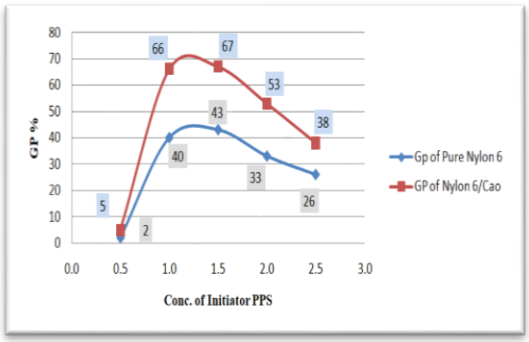

Fig 3. Effect of initiator concentration

Effect of Temperature

The effects of reaction temperature on the grafting yield were examined in the range of 40°C- 80°C keeping the monomer concentration constant at 15%, emulsifier concentration constant as 2.5% and the initiator concentration as constant at $1.5x10^{-3}$ (mol/l) for 4 hr grafting time. **Figure 4** shows the effects of temperature on the grafting yield of PA6-gAA and PA6/CaO-gAA. The temperature of the grafting medium is one of the most critical reaction parameters that influence the grafting yield during the preparation of grafted polymers. According to the figure, increasing the temperature of the grafting mixture to 60°C significantly enhances the degree of grafting. The increase in grafting yield with increasing temperature can be attributed to (i) increased initiator and monomer mobility (ii) increased rate of initiator and monomer diffusion from the solution phase to the nanofibers backbone (iii) increased number of active sites in the reaction medium (iv) increased rate of initiation and propagation step (v) increased

swellability of nanofibers [30]. But the grafting yield decreases when the temperature rises above 60°C. This is because higher temperatures result in higher monomer combination rates, which increases homopolymerisation reaction and decreases grafting yield [31].

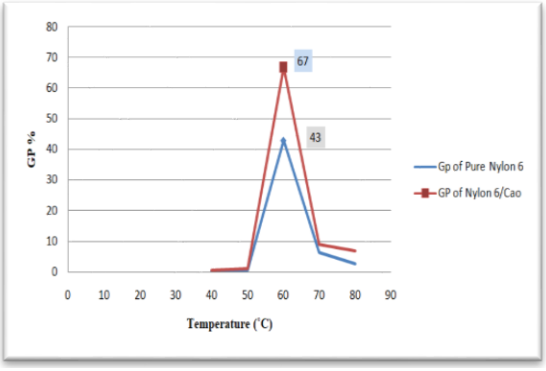

Fig 4. Effect of Temperature

Scanning Electron Microscope (SEM)

The morphology of the prepared samples was investigated by SEM at X100 um magnification.

Before modification SEM micrographs of pure PA6 and PA6-CaO electronspun nanofibers membranes are shown in **figure 5**. The produced PA6-CaO shows that the existence of CaO with PA6 improved the characteristics of the resultant nanofibers, which indicated uniformly smooth and continuous nanofibers with a homogeneous dispersion without any CaO agglomeration in the polymer matrix [32].

After modification the grafted PA6-gAA and PA6/CaO-gAA micrographs are illustrated in **figure 6**. From the figure it is clear that, the unmodified nanofibers were fully separated from each, but with the AA grafted surface modified sample a rough and irregular surface of modified PA6 nanofibrous membrane was observed. The SEM images additionally show that the modification process did not affect the fibrous structure of PA6 nanofibers or the formation of a fiber network between PA6 and poly AA during the graft polymerization process, confirming that AA was successfully attached to PA6 nanofibers. It was also reported that grafting PA6 nanofibers with AA resulted in an increase in diameter and the formation of a heterogeneous plateau [33]. On the other hand from the figure find that the presence of CaO nanoparticles plays an important role in the enhancement of fibrous membrane, where a full fibrous membrane was obtained after modification by AA through grafting polymerization in the case of PA6/ CaO electrospun fibre [34].

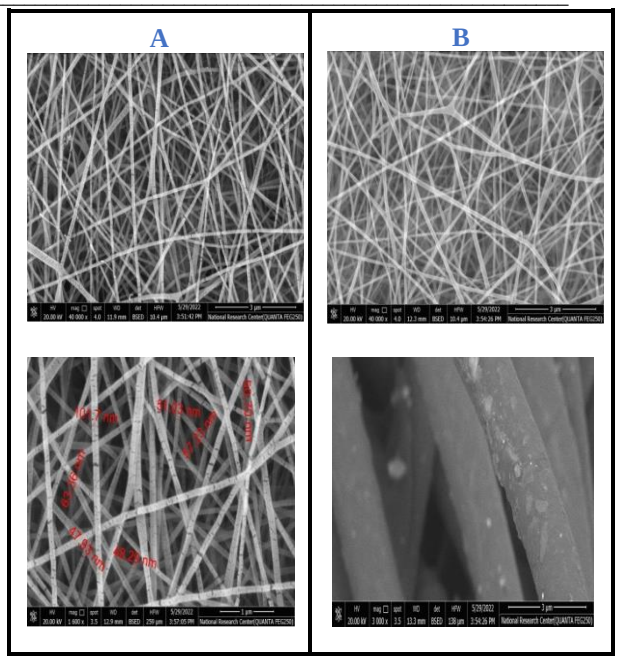

Fig 5. SEM image for A) Pure PA6 and B) PA6/CaO nanocomposite.

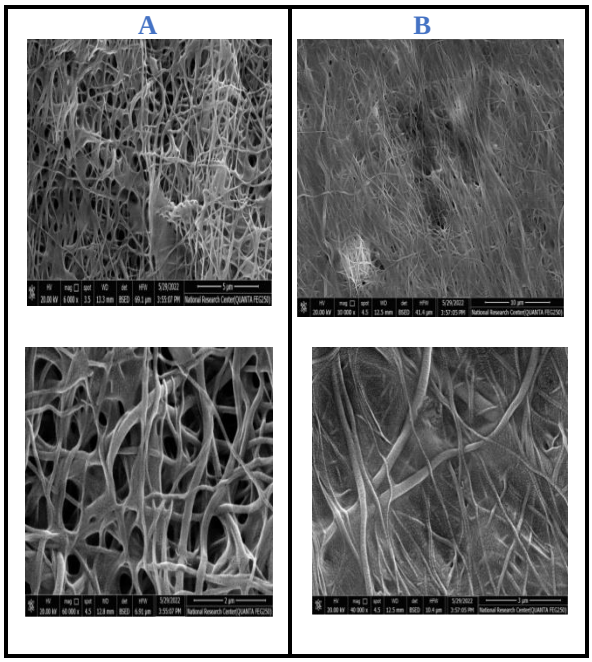

Fig 6. SEM image for A) grafted PA6-gAA and B) PA6/CaO-gAA

Swelling behavior

PA6-gAA and PA6/CaO-gAA have the ability to swell and hold a lot of liquid in their network structure. The nanofibrous mat also has a greater surface area, which increases wettability and absorption. As a result, the weights of swollen nanofiber membrans were calculated at various time periods, and the swelling ratio was reported. **Figure 7** shows the variation in swelling ratio over time for PA6-gAA and PA6/CaO-gAA nanofibrous mats. It can be noticed that, the swelling ratio increased significantly with time,

reaching 70% for PA6-gAA and 85% for PA6/CaO-gAA in approximately 24 hours [35].

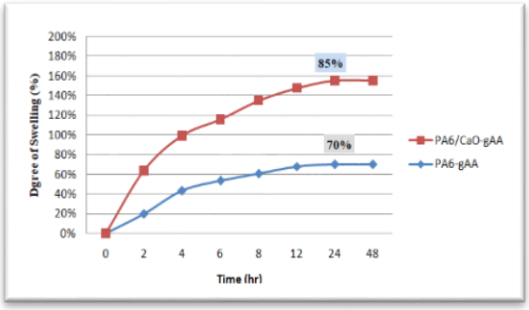

Fig 7. Absolute Swelling behavior of PA6-gAA and PA6/CaO-gAA

FT-IR characterization

The formation of graft copolymer of PA6 and PA6/CaO nanofibrous membrane with acrylic acid monomer were confirmed through FT-IR analysis. The FT-IR spectrums of PA6 and PA6/CaO before and after grafting were shown in the **figure 8 (a&b).**

From **Figure 8** it shown IR spectrum of pure PA6 and PA6/CaO observed that the appearance of strong band at 3296 cm^{-1} which corresponding to the stretching vibration of N-H group which appeared sharper and more visible due to the higher formic acid content [36]. Also the band observed at 2935 cm^{-1} and 1641 cm^{-1} due to the stretching vibration of CH_2 of aliphatic group, stretching vibration of C=O in secondary amide. The band at 1500 cm^{-1} attributed to the bending vibration of N-H group. Whereas in the spectrum of the graft copolymer PA6-g-AA and PA6/CaO-gAA besides retaining the above mentioned bands of PA6 and PA6/CaO , it shows an additional stronger absorption of band at 1730 cm^{-1} , 1162 cm^{-1} corresponding to the stretching vibration of carbonyl group and stretching of C-O of acid. The previous peaks were absent from the FT-IR spectrum of pure PA6 or PA6/ CaO before grafting that confirms that the grafted of acrylic acid monomer in PA6 or PA6/CaO effectively. In addition to the above bands PA6/ CaO and PA6/CaO-gAA has a significantly sharper and higher peaks as well as a visible strong absorption band at 1454 cm^{-1} corresponding to the calcium oxygen bond, which is not visible in the pure PA6 and PA6-g-AA IR figure [37, 38].

Thermogravimetric analysis (TGA)

The TGA thermography features of PA6 and PA6/CaO before and after grafting are depicted in **figures 9 and 10**, respectively. Figure 9 shows that the PA6 binary fiber showed one-step degradation transition, which Around 91% of the sample had disintegrated at the end of the experiment leaving behind 9 % of the sample remained as a residue at 597°C ; additionally, The PA6-gAA grafted fiber showed two-step degradation transition, which can be obviously seen in forms of weight losses at temperature ranges of 200–317 and 317– 597 ºC, the maximum weight loss occurs at first step , Around 74 % of the sample is disintegrated in 597`C leaving behind 26% of the sample as a residue. The PA6/CaO sample, on the other hand, had around 86 percent of the sample disintegrate in a single step, leaving about 14% of the sample as a residue at 597 ºC. While; The PA6/CaO-gAA grafted fiber had deteriorated with 71% of the sample in two steps at 597 ºC, leaving 29% of the sample as a residue.

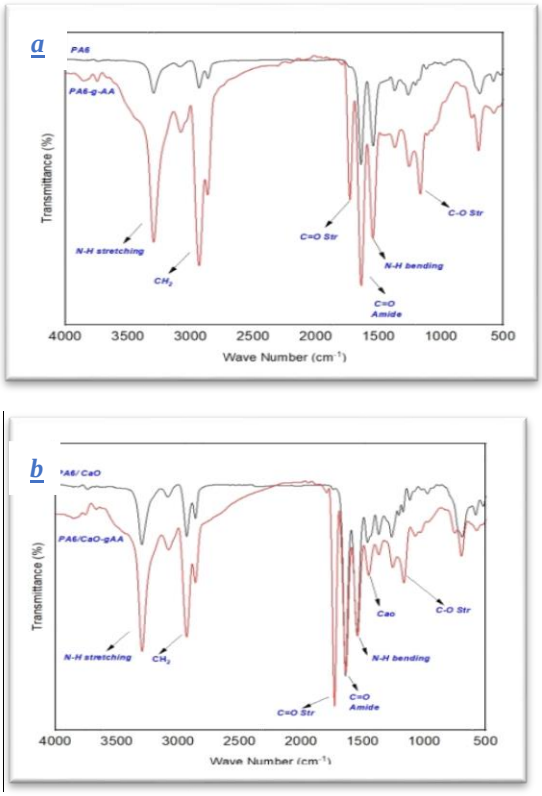

Fig 8. FT-IR for a) Pure PA6 and b) PA6/CaO nanocomposite before and after grafting

According to the previous results, it was concluded that the PA6-graft copolymer has higher thermal stability than the engrafted polymer; and when comparing Figure.9 with Figure.10, it was found that the PA6/CaO-gAA sample was observed to be highly thermal stable, which was confirmed by the amount of grafted sample that remained as residue at the end of the experiment and the various decomposition temperatures.

Differential Scanning Calorimetry (DSC)

Figures 11–12 represent the DSC curves of PA6 and PA6/CaO before and after grafting. Broad endothermic peaks are observed at various temperatures, indicating the crystallisation of the samples. **Figure 11** shows a sharp endothermic peak at 257 0C, while the DSC curve of PA6-gAA shows a sharp and broad endothermic peak at 259 ºC. On the other hand, **figure 12** shows that two broad endothermic peaks are obtained at 49 ºC and 258 ºC

showing the recrystallizaion process of PA6/CaO at different temperatures. The DSC curve of PA6-CaO-gAA showed two sharp and broad endothermic peaks were observed at 56 ºC and 264 ºC.

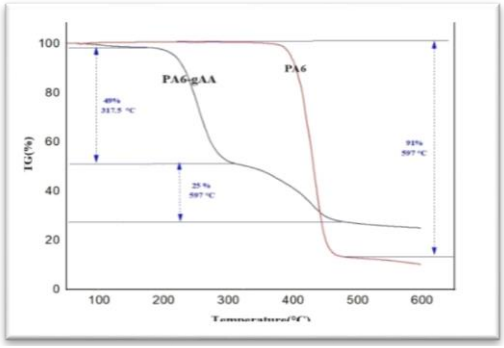

Fig 9. TGA curve of PA6 and PA6-gAA

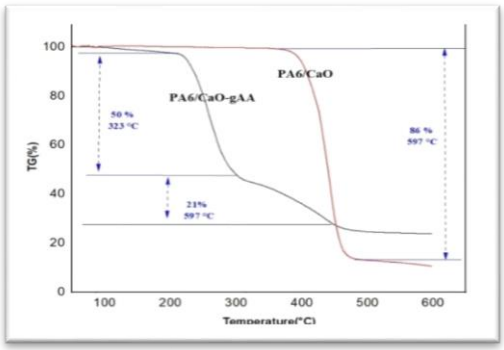

Fig 10. TGA curve of PA6/CaO and PA6/CaO-gAA

On comparing the DSC curves of samples, it was observed that the endothermic peaks are shifted to higher values. This concluded that the grafting of AA to PA6 and PA6/CaO increases the thermal stability.

Application of prepared grafted polymer onto metal uptake

The sorption capacity of the prepared AA surface modified PA6/CaO Electrospun nanofibrous membranes was investigated for use in the removal of heavy metal (Co^{+2} & Cr^{+6}) from Simulated aqueous solution under various conditions, including initial metal concentration ; PH ; contact time and temperature.

Calibration curve

One of the most commonly used calibration analyses is linear regression. The calibration curve is used to assess the accuracy of the result once the relationship between the input value and the response value, which is expected to be represented by a straight line, has been established. According to the calibration curve in **figure 13,** there is an approximate linear connection between absorbance and Co^{+2} ; Cr^{+6} content in aqueous solutions. The regression coefficient (R^2) is found to be quite strong, with values of 0.998 and 1 for Co^{+2} and Cr^{+6}, respectively.

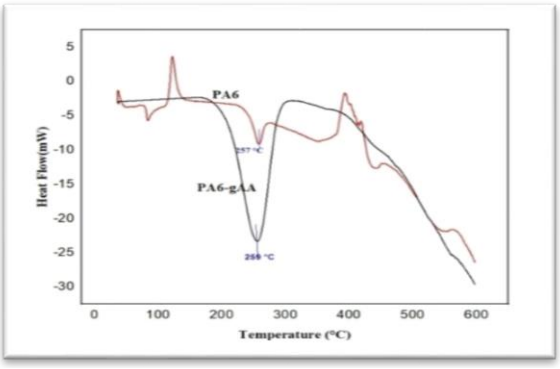

Fig 11. DSC curve of PA6 and PA6-gAA

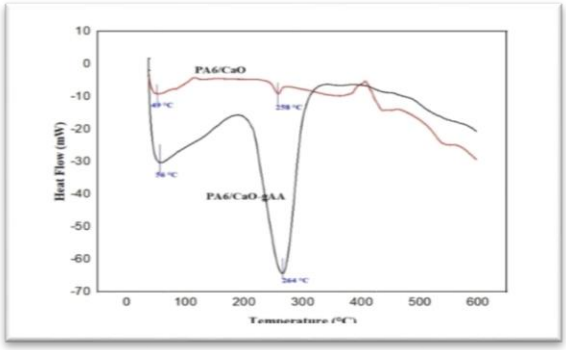

Fig 12. DSC curve of PA6/CaO and PA6/CaO-gAA

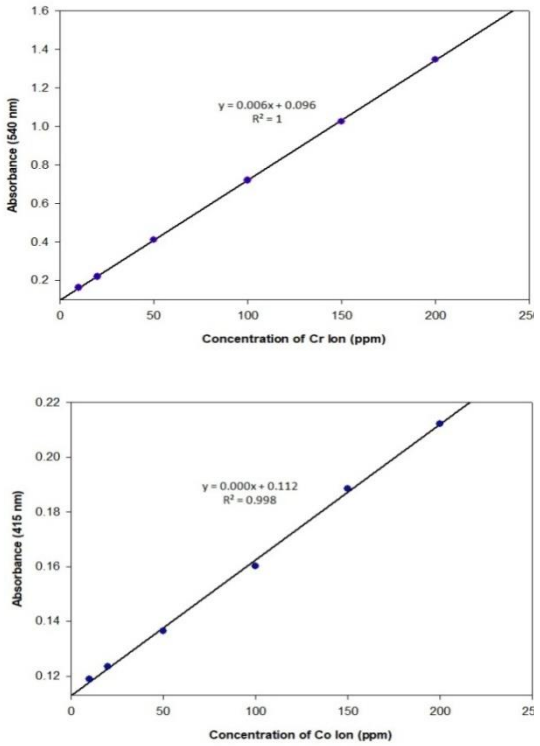

Fig 13. Calibration curve of Cobalt & Chromium Adsorption

Effect of initial concentration

Figure 14 illustrates the effect of initial cobalt and chromium concentrations on cobalt and chromium removal when concentrations range from 10 to 200 ppm under operating conditions of 24 hour magnetic stirring, 30 mg of PA6/CaO-gAA /20 mL of adsorbate, and a constant pH of 7 at room temperature. The results showed a gradual decline in cobalt and chromium removal when the concentration of cobalt and chromium in the solution was raised. So, at 10 ppm, the results showed that approximately 86% and 60% of cobalt and chromium were removed, respectively. This decline was caused by a high ratio of the number of metal ions present in solution to the number of functional adsorption sites on the grafted polymer as the metal concentration increased [39].

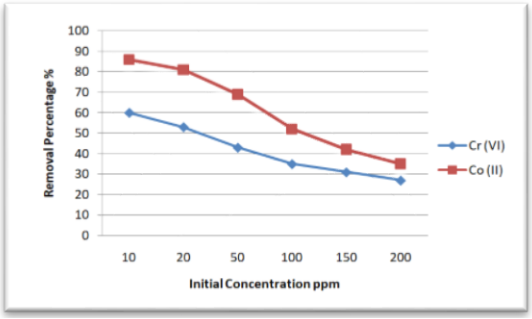

Fig 14. Effect of initial concentration (ppm)

Effect of solution pH

When using PA6/CaO-gAA to remove cobalt and chromium ions from solutions, the impact of solution pH was evaluated in the pH range 2–7 with a constant PA6/CaO-gAA amount of 30 mg/20 mL of adsorbate, a magnetic stirring time of 24 hours, and a metal ions concentration of 10 ppm, pH adjustments were carried out at room temperature using 0.1 N HCl and 0.1 N NaOH. The proportion of cobalt and chromium removed at varying solution pH is shown in **Figure 15**. At pH 2, the least amount of cobalt and chromium was removed. The percentage of cobalt and chromium removed increased as the pH of the solution increased; up to pH 5.This could be due to the large number of active surface sites of PA6/CaO-gAA. As a result, at low pH, it may become more positively or less negatively charged, increasing the competition for available adsorption sites between H^+ and metal ions [40]. As pH increases, however, competition declines as these surface active sites become more negatively charged, enhancing the adsorption of positively charged metal ions via electrostatic attraction. Moreover, increasing the pH above pH 5 causes metal precipitation and accumulation due to the creation of soluble hydroxyl complexes, which causes the adsorption process to deteriorate [41,42].

Effect of contact time

Figure 16 shows the effect of contact time on cobalt and chromium adsorption by PA6/CaO-gAA was studied by varying the contact time of magnetic stirring between the adsorbate and adsorbent in the range of 20–360 min with a constant PA6/CaO-gAA amount of 30 mg/20 mL of adsorbate and a metal ions concentration of 10 ppm at room temperature, while the solution's pH was kept constant at pH 5. The results revealed that the adsorption of cobalt and chromium ions on PA6/CaO-gAA is rather quick, with equilibrium being obtained in 150 minutes [43]. Due to the obvious adsorption of cobalt and chromium on the surface Active sites of PA6/CaO-gAA, the adsorption process was initiated rapidly at the start of the reaction. While increasing contact time did not increase absorption, the equilibrium was attained due to a decrease in widely available active sites for metal ion binding. The adsorption did not continue after 150 minutes of contact and remained steady until 360 minutes [44].

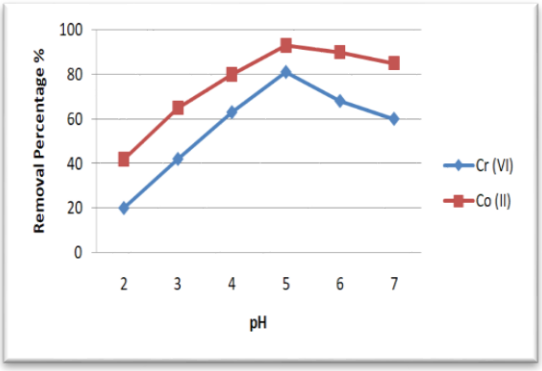

Fig 15. Effect of pH

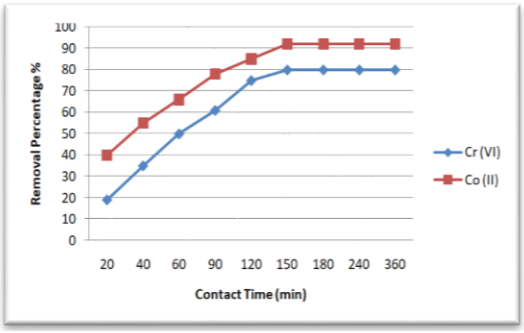

Fig 16. Effect of Contact Time (min)

Effect of Temperature

The effect of temperature on adsorption has been studied in the range of 30 to 70°C with a constant PA6/CaO-gAA amount of 30 mg/20 mL of adsorbate, a metal ions concentration of 10 ppm at pH 5, and a constant magnetic stirring time of 150 min, and the effect of temperature on cobalt and chromium adsorption is shown in **figure 17**. At 30°C, the optimum adsorption of cobalt and chromium ions is seen, after which the removal adsorption decreases as the solution temperature increases. When the

temperature increases, the metal ions become more mobile and the retarding forces acting on the diffusing ions decrease [45]. On the other hand, attractive forces between the active sites on the PA6/CaO-gAA surface and metal ions are weakened and then sorption reduced. In contrast, in endothermic adsorption investigations, the increase in temperature not only increases the rate of diffusion of the metal ions present in the bulk solution to the adsorbent surface but also increases the rate of complexation with the functional groups present in the adsorbent [46,47].

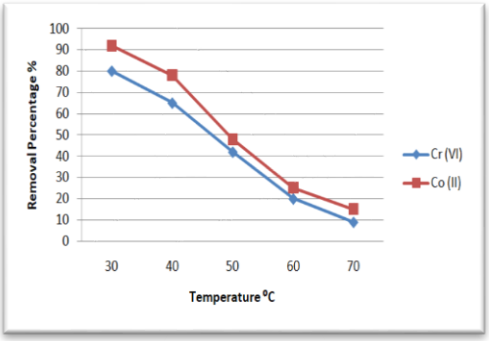

Fig 17. Effect of Temperature (ºC)

Adsorption isotherms models

Adsorption is a dynamic process that is typically characterised by isotherms [48], which are obtained by fitting mathematical models to experimental data. The Langmuir [49] and Freundlich [50] adsorption isotherm models were used to investigate the adsorption isotherms of Co^{2+} and Cr^{6+} ions onto PA6/CaO-gAA surfaces. The Langmuir and Freundlich isotherm models are the simplest and most commonly used isotherms to represent the adsorption of components from a liquid phase onto a solid phase. These models were tested to determine the maximal capacity of cobalt and Chromium removal using PA6/CaO-gAA polymer. The quality of the isotherm fit to the experimental data was traditionally judged by the magnitude of the regression's correlation coefficient, i.e., the isotherm with the R2 value closest to unity was considered to be the ideal suitable. The adsorption isotherms for cobalt and chromium removal were studied using the best conditions obtained from experimental work with a constant PA6/CaO-gAA amount of 30 mg/20 mL of adsorbate, a metal ions concentration of 10 ppm at pH 5, and a constant magnetic stirring time of 150 min, and the temperature of the solution was 30°C. Afterword; The Langmuir and Freundlich isotherms were used to fit the obtained data [51].

The Langmuir isotherm model

The Langmuir adsorption isotherm model is one of the earliest theoretical treatments of non-linear sorption, suggesting that uptake proceeds on a homogeneous surface via monolayer sorption with no interaction between the adsorbed molecules [52]. The linear form of the Langmuir adsorption isotherm is represented as:

$$\frac{C_e}{q_e} = \frac{1}{bq_{\max}} + \frac{C_e}{q_{\max}}$$

Where $\mathbf{C_e}$ is the cobalt and chromium ion equilibrium concentration (mg/L); $\mathbf{q_e}$ is amount of cobalt and chromium ions adsorbed per unit weight of adsorbent (mg/g); $\mathbf{q_{max}}$ is amount maximum adsorption capacity referred to the mount of Cr^{+6} and Co^{+2} required to occupy all the available site per unit mass of sample (mg/g); **b** is the adsorption equilibrium constant (L/mg). The both data obtained from linear Langmuir isotherm plot for the adsorption of cobalt and chromium onto PA6/CaO-gAA Surface are presented in **Table 1** and plotted in **Figure 18.**

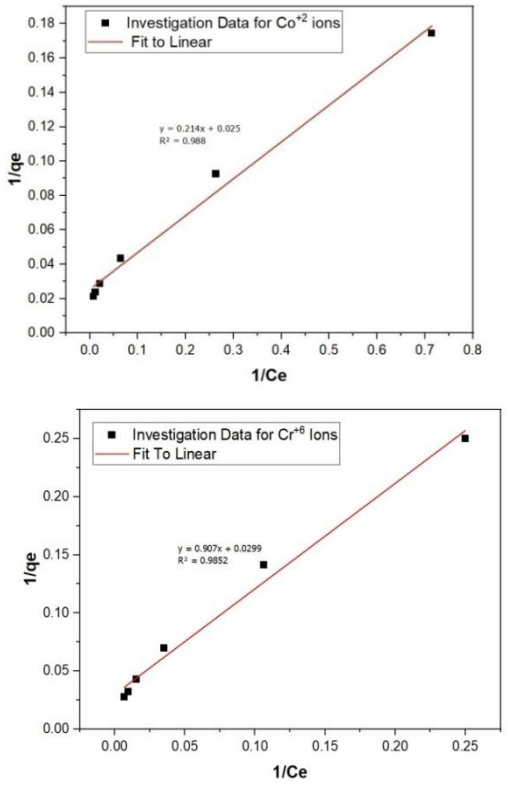

Fig 18. Langmuir Plot for adsorption of Co^{2+} & Cr^{6+} on PA6/CaO-gAA Surface

The Freundlich isotherm model

Freundlich adsorption isotherm model can be applied for non-ideal sorption onto heterogeneous surfaces involving multilayer sorption. The linearized Freundlich isotherm model was applied for the adsorption of cobalt and chromium is expressed as:

$$\log q_e = \log K + \frac{1}{n}\log C_e$$

Where $\mathbf{q_e}$ (mg/g) is the amount of cobalt and chromium adsorbed per gram of the adsorbent at equilibrium, $\mathbf{C_e}$ (mg/L) is the equilibrium concentration of the adsorbate in solution, where **k** and **n** are the constant characteristics of the system

affecting the adsorption process (adsorption capacity and intensity). The applicability of the Freundlich adsorption isotherm was also analyzed, using the same set of experimental data, by plotting log (q_e) versus log (C_e). The data obtained from linear Freundlich isotherm plot for the adsorption of cobalt and chromium onto PA6/CaO-gAA Surface are presented in **Table.1** and plotted in **Figure 19**. The value of **n** between 1 and 10 shows a good adsorption which indicates that cobalt and chromium are favorably adsorbed by PA6/CaO-gAA [53].

The experimental data obtained From Both Isotherm models for Two metal were correlated very well to the Langmuir model and Freundlich isotherm model based on R^2 values indicating homogeneous distribution of adsorptive sites and monolayer adsorption [54].

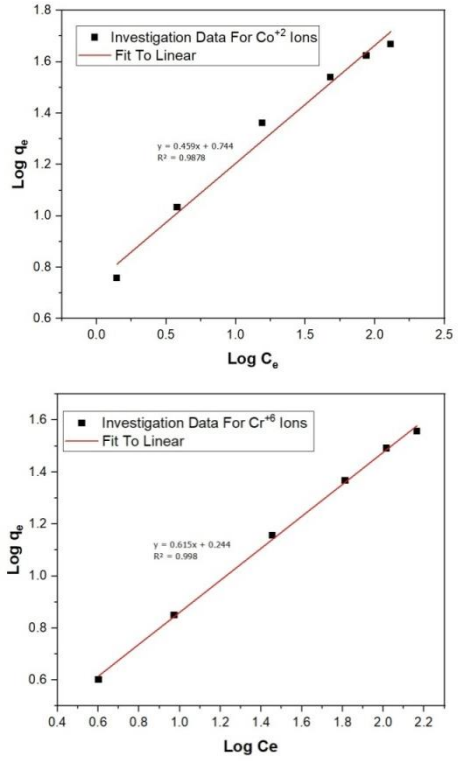

Fig 19. Freundlich Plots for adsorption of Co^{+2} & Cr^{+6} on PA6/CaO-gAA Surface

Table 1: Langmuir and Freundlich parameters for adsorption of Co (II) & Cr (VI)

Model	Isotherm parameters	Co (II) Ions	Cr (VI) Ions
Langmuir	q_{max} (mg//g)	39	33
	b (L/mg)	0.1186	0.033
	R^2	0.98617	0.988
Freundlich	n	2.18	1.63
	K_f	5.54625	1.753881
	R^2	0.9789	0.99828

Conclusion

Based on the results presented in this paper, we conclude that Polyamide 6 (PA6) electrospun nanofibrous membranes were successfully prepared with a concentration of 30% (wt/v) and Polyamide 6 nanofibers containing calcium oxide nanoparticles (PA6/CaO) were obtained with a CaO concentration of 1% (wt/wt) by electrospinning of polymer solution. To obtain the best grafting conditions, the obtained PA6 and PA6/CaO electrospun membranes were modified by grafting polymerization with AA monomer with various synthetic parameters. The following are the optimal grafting conditions based on the preceding findings: At 60 °C, the acrylic acid concentration was 15%, the surfactant concentration was 2.5 %, and the initiator concentration was $1.5x10^{-3}$ (mol/l) with PA6/CaO-gAA nanofibers.

The proof of grafting was obtained from the FT-IR; thermal behavior was confirmed through DSC and TGA results, the morphology of prepared polymers studied through SEM images revealed that the PA6 fibers and the modified PA6/CaO-gAA electrospun membrane surface were smooth and continuous nanofibers with a slight increase in the nanofibers diameters.

The maximum swelling was found to be 85% of PA6/CaO-gAA and 70% of PA6-gAA in 24 hours in distilled water at a temperature of 30°C, according to the swelling behavior of identified samples of PA6-gAA and PA6/CaO-gAA with high grafting proportion as a function of time. As the time is prolonged, the swelling percentage doesn't really change.

The produced modified nanofibrous membranes of PA6/CaO-gAA were used in adsorption and the removal of heavy metals (Co^{2+}; Cr^{6+}) from simulated water solutions under different initial concentrations, pH values, temperature, and contact time, and the results showed that the optimum conditions for metal removal were metal concentration of 10 ppm, pH 5, for 150 min under a temperature of 30 ^{0}C, while Co^{2+} showed higher diffusion capacity than Cr^{+6} on grafted fibre surface, which reached 92% and 80 % in Co^{2+} and Cr^{6+}, respectively.

References

1- Sriyanti I., Agustini M .P., Jauhari J., Sukemi, Nawawi Z., Electrospun Nylon-6 Nanofibers and Their Characteristics., *Jurnal Ilmiah Pendidikan Fisika Al-BiRuNi*,9: 9-19 **(2020)**.

2- Sriyanti I., Edikresnha D., Rahma A., Miftahul Munir M., Rachmawati H., Khairurrijal K., Correlation between Structures and antioxidant activities of polyvinylpyrrolidone/garcinia mangostana L. extract composite nanofiber mats prepared using electrospinning., *Journal of Nanomaterials*, Article ID 9687896, 10 pages **(2017)**.

3- Ismar E., Karazehir T., Ates M., Sarac A. S., Electrospun carbon nanofiber web electrode: Supercapacitor behavior in various electrolytes., *Journal of Applied Polymer Science*, 135: 1–10 **(2018)**.

4- Quirós J., Borges J. P., Boltes K., Rodea-Palomares I., Rosal R., Antimicrobial electrospun silver-, copper- and zinc-doped polyvinylpyrrolidone nanofibers., *J. Hazard. Mater*, 299: 298-305 **(2015)**.

5- Subbiah T., Bhat G.S., Tock R.W., Parameswaran S., Ramkumar S.S., Electrospinning of nanofibres., *J Appl Polym Sci*, 96:557–569 **(2005)**.

6- Zuo W., Zhu M., Yang W., Yu H., Chen Y., Zhang Y., Experimental study on relationship between jet instability and formation of beaded fibres during Electrospinning, *Polym Eng Sci*, 45:704–9 **(2005)**.

7- Huang Z.M., Zhang Y.Z., Kotaki M., Ramakrishna S., Characterization of the Surface Biocompatibility of the Electrospun PCL-Collagen Nanofibers Using Fibroblasts., *Compos. Sci. Technol*. 6:2583-2589 **(2003)**.

8- Wannatong L., Sirivat A., Supaphol P., Effects of solvents on electrospun polymeric fibers: preliminary study on polystyrene., *Polym. Int*., 53:1851- 1859 **(2004)**.

9- Ghani M., Gharehaghaji A. A., Arami M., Takhtkuse N., Rezaei B., Fabrication of Electrospun Polyamide-6/Chitosan Nanofibrous Membrane toward Anionic Dyes Removal., *Journal of Nanotechnology*., Article ID 278418, 12 pages **(2017)**.

10- Singh G., Rana D., Matsuura T., Ramakrishna S., Narbaitz R. M., Tabe S., "Removal of disinfection byproducts from water by carbonized electrospun nanofibrous membranes., *Separation and Purification Technology*, 74: 202–212 **(2010).**

11- Mit-uppatham C., Nithitanakul M., Supaphol P., Ultrafine Electrospun Polyamide- 6 Fibers: Effect of Solution Conditions on Morphology and Average Fiber Diameter., Macromol. *Chem. Phys*., 205: 2327–2338 **(2004)**.

12- Dong A., Xie J., Wang W., Yu L., Liu Q., Yin Y., A novel method for amino starch preparation and its adsorption for Cu (II) and Cr (VI). *J Hazard Mater*, 81:448-454 **(2010)**.

13- Liu Y. C., Wang J. S., Huang K. L., Xu W., Graft copolymers of poly(methyl methacrylate) and polyamide-6 via in situ anionic polymerization of e-caprolactam and their properties., *Polym. Bull*., 64:159–169 **(2010)**.

14- Ting T.M., Nasef M. M., Hashim K., Modification of nylon-6 fibres by radiation-induced graft polymerisation of vinylbenzyl chloride, *Radiation Physics and Chemistry*.,109:54-62 **(2015)**.

15- Patra J. M., Panda S. S., Dhal Dong N. K., Biochar as a low-cost adsorbent for heavy metal removal: A review., *J. M. Patra al. Int. J. Res. Biosciences*, 6: 1-7 **(2017)**.

16- Yasmeen S., Kabiraz M.K., Saha B., Qadir M.D., Chromium (VI) Ions Removal from Tannery Effluent using Chitosan-Microcrystalline Cellulose Composite as Adsorbent., *International Research Journal of Pure & Applied Chemistry* 10: 1-14 **(2016)**.

17- Abdel-Halim E.S., Al-Deyab S.S., Chemically modified cellulosic adsorbent for divalent cations removal from aqueous solutions., *Carbohydrate Polymers*, 87:1863-1868 **(2012).**

18- Wu S. Y., Xu Q., Chen T.S., Wang M., Yin X. Y., Ni-Ping Zhang N. p., Shen Y.Y., Determination of Bisphenol A in Plastic Bottled Drinking Water by High Performance Liquid Chromatography with Solidmembrane Extraction Based on Electrospun Nylon 6 Nanofibrous Membrane, *Chin J Anal Chem*, 38: 503-507 **(2010)**.

19- Bukhari A.A.H., Monier M., Elsayed N. H., Surface molecular imprinting of nylon fibers for chiral recognition of D-phenyllactic, *Polym Int*, 68:1460–1467 **(2019)**.

20- Gulsonbi M., Parthasarathy S., Raj K. B., Jaisankar V., Green synthesis, characterization and drug delivery applications of a novel silver / carboxymethylcellulose – poly (acrylamide) hydrogel nanocomposite. Ecotoxicology and Environmental Safety, 134: 421–426 **(2016)**.

21- Qiao Z., Tran L., Parks J., Zhao Y., Hai N., Zhong Y., Ji H. F., Highly stretchable gelatinpolyacrylamide hydrogel for potential transdermal drug release. *Nano Select*, 2: 107– 115 **(2021)**.

22- Metwally B.S., El-Sayed A. A., Radwan E.K., Hamouda A.S., El-Sheikh M.N., Salama M., Fabrication, characterization, and dye adsorption capability of recycled modified polyamide nanofibers, *Egypt .J. Chem*, 61:867-882 **(2018)**.

23- Lide D. R., CRC Handbook of Chemistry and Physics. 88 ed. Taylor & Francis LLC, London: Editors Lide; **(2007)**.

24- Sobh R. A., Ekram B., Mohamed W. S., Fabrication of Acrylic Modified Surface of Polyamide 6/CaO Electrospun Nanofibrous Membrane for Effective Dye Removal., *Egypt.J.Chem*.63: 2249 - 2260 **(2020)**.

25- El-Feky G. S., Sharaf S. S., El Shafei A. and Hegazy A. A. Using chitosan nanoparticles as drug carriers for the development of a silver sulfadiazine wound dressing, *Carbohydrate. Polymers*, 158: 11- 19 **(2017)**.

26- Lakshmi. P., Vijayalakshmi. K., Sudha P. N., Synthesis and characterization of graft copolymers of nylon 6 with maleic anhydride and methylmethacrylate., *Arch. Appl. Sci. Res*., 3:351-363 **(2011)**.

27- Li X., Gu X., Zhang S., Li H., Feng Q., Sun J. and Zhao Q., Improving the fire performance of nylon 6,6 fabric by chemical grafting with acrylamide. Industrial and Engineering Chemistry Research, 52:2290–2296 **(2013)**.

28- Shaffei K. A., Moustafa A. B., Mohamed W. S., Grafting Emulsion Polymerization of Glycidyl Methacrylate onto Leather by Chemical Initiation Systems., *Journal of Applied Polymer Science* 109:3923-3931 **(2007)**.

29- Lee D. J., Lee S., Kim I. W., Effects of Humidity and Surfaces on the Melt Crystallization of Ibuprofen., *Int. J. Mol. Sci*. 13:10296- 10304 **(2012)**.

30- Sehgal T., Rattan S. Synthesis, Characterization and Swelling Characteristics of Graft Copolymerized Isotactic Polypropylene Film., *International Journal of Polymer Science*., Article ID 147581 **(2010)**.

31- Sun T., Xu P., Liu Q., Xue J., Xie W., Graft copolymerization of methacrylic acid onto carboxymethyl chitosan., *European Polymer Journal*, 39:189–192 **(2003)**.

32- Smart G., Kandola B.K., Horrocks A.R., Nazare S., Marney D., Characterisation of the dispersion in polymer flame retarded nanocomposites. *Polym. Adv. Technol*. 44: 1631-1641 (**2008)**.

33- Kayaci F., Aytac Z., Uyar T., Surface modification of electrospun polyester nanofibers with cyclodextrin polymer for the removal of phenanthrene from aqueous solution., *Journal of Hazardous Materials*, 261:286-294 **(2013)**.

34- Wang J., Zhang P., Liang B., Liu Y., Xu T., Wang L., Cao B. and Pan K., Graphene Oxide as an Effective Barrier on a Porous Nanofibrous Membrane for Water Treatment, *ACS Appl. Mater. Interfaces*, 8: 6211-6218 **(2016)**.

35- Díaz -guerrero A., Castillo-miranda C., Peraza-vázquez H., Modelling of acetaminophen release from hydroxyethylcellulose/ polyacrylamide hydrogen., *Mater. Res.*, Express 8, 015310 **(2021).**

36- Parlay, Ş., Avc, A., Pehlivan E., Electrospinning of polymeric nanofiber (nylon 6, 6 / graphene oxide) for removal of Cr (VI): synthesis and adsorption studies., *Journal of Analytical Science and Technology*, 10:13 **(2019).**

37- Fan, Q., Yang, Y., Ugbolue S.C., Wilson, A.R., Dyeable polypropylene via nanotechnology., *National Textile Center* **(2008).**

38- Sheela B., Kalaiarasi K., Vijayalakshmi K. and Sudha P. N., Optimization of Grafting Parameters of Nylon6-Graft-Acrylic Acid Copolymer Using Ceric Ammonium Nitrate as an Initiator., *International Journal of Applied and Advanced Scientific Research*, 1: 9-16 **(2016)**.

39- Manohar D.M., Noeline B.F., Anirudha T.S., Adsorption performance of Al-pillared bentonite clay for the removal of cobalt(II) from aqueous phase., *Applied Clay Science.*, 31: 194-206 **(2006)**.

40- Unuabonah E.I., Adebowale K.O., Olu-Owolabi B.I., Yang L.Z., Kong L.X., Adsorption of Pb(II) and Cd(II) from aqueous solutions onto sodium tetraborate-modified kaolinite clay: equilibrium and thermodynamic studies, *Hydrometallurgy* 93: 1–9 **(2008)**.

41- Ghassabzadeh H., Torab-Mostaedi M., Mohaddespour A., Maragheh M.G., Ahmadi S.J., Zaheri P., Characterizations of Co (II) and Pb (II) removal process from aqueous solutions using expanded perlite. Desalination, 261: 73-79 **(2010)**.

42- Sewvandi G.A., Adikary S.U., Removal of heavy metals from waste water using chitosan. *Management Systems Internet Journal*., **(2011)**.

43- Sh M., Yu A.P., Ren Ch. L., Chen Y.X., Chen X., Effect of pH, ionic strength and fulvic acid on the sorption and desorption of cobalt to bentonite, *Appl. Radiat. Isotopes* 64:455–461 **(2006)**.

44- Chattopadhyay D.P., Inamdar M.S., Aqueous behaviour of chitosan. *International Journal of Polymer Science*., 1-7 **(2010)**.

45- El-Shafey E., Behavior of reduction-sorption of chromium (VI) from an aqueous solution on a modified sorbent from rice husk. *Water Air Soil Poll.,* 163: 81-102 **(2005)**.

46- Tizro S., Baseri H., Removal of Cobalt Ions from Contaminated Water Using Magnetite Based Nanocomposites: Effects of Various Parameters on the Removal Efficiency J. Water Environ. *Nanotechnol.*, 2; 174-185 (**2017**).

47- Kannamba B., Laxma K., Rao B.V., Removal of Cu(II) from aqueous solutions using chemically modifi ed chitosan, *J. Hazard. Mater*., 175: 939–948 **(2010)**.

48- Vareda, J. P., Valente A. J. M., Duraes L., Heavy metals in Iberian˜ soils: Removal by current adsorbents/amendments and prospective for aerogels. *Adv. Colloid Interface Sci*., 237:28−42 **(2016)**.

49- Langmuir I., The adsorption of gases on plain surface of glass, mica and platinum, *J. Am. Chem. Soc*., 40:1361 **(1918)**.

50- Freundlich H., Uber die adsorption in losungen, *Z. Phys. Chem*. 57:385-471 **(1906)**.

51- Nadaroglu H., Kalkan E., Removal of cobalt (II) ions from aqueous solution by using alternative adsorbent industrial red mud waste material, *international Journal of Physical* Sciences., 7:1386 -1394 **(2012)**.

52- Bansal M., Sing D., Garg V.K., Rose P. Use of agricultural waste for the removal of nickel ions from aqueous solutions: Equilibrium and kinetic studies. World Acad. *Sci. Eng. Technol*., 51: 431-437 **(2009)**.

53- Al-Shahrani S.S., Treatment of wastewater contaminated with cobalt using Saudi activated bentonite, *Alexandria Engineering Journal*., 53, 205-211 **(2014)**.

54- Avila M., Burks T., Akhtar F , Göthelid M., Lansåker P. C., Toprak M.S., Muhammed M., Uheida A. ; Surface functionalized nanofibers for the removal of

chromium(VI) from aqueous solutions; *Chemical Engineering Journal;* 245: 201-209 **(2014)**.